Molecular Therapy
Methods & Clinical Development
Original Article

Site-Specific Glycation and Chemo-enzymatic Antibody Sortagging for the Retargeting of rAAV6 to Inflamed Endothelium

Hannah A. Pearce,[1,2] Hongwei Qian,[3,4] Timothy U. Connell,[5] Dexing Huang,[2] Claudia Gottstein,[6] Paul S. Donnelly,[5] Karlheinz Peter,[2] Paul Gregorevic,[3,4,7,8] and Christoph E. Hagemeyer[1]

[1]NanoBiotechnology Laboratory, Monash University, Melbourne, VIC, Australia; [2]Atherothrombosis and Vascular Biology Laboratory, The Baker Heart and Diabetes Institute, Melbourne, VIC, Australia; [3]Muscle Research and Therapeutics Laboratory, The Baker Heart and Diabetes Institute, Melbourne, VIC, Australia; [4]Centre for Muscle Research, Department of Physiology, University of Melbourne, Melbourne, VIC, Australia; [5]School of Chemistry, Bio21 Molecular Science Institute, University of Melbourne, Melbourne, VIC, Australia; [6]Neuroscience Research Institute, University of California, Santa Barbara, Santa Barbara, CA, USA; [7]Department of Biochemistry and Molecular Biology, Monash University, Australia; [8]Department of Neurology, University of Washington School of Medicine, Seattle, WA, USA

Gene therapy holds great potential for conditions such as cardiovascular disease, including atherosclerosis and also vascular cancers, yet available vectors such as the adeno-associated virus (rAAV) transduce the vasculature poorly. To enable retargeting, a single-chain antibody (scFv) that binds to the vascular cell-adhesion molecule (VCAM-1) overexpressed at areas of endothelial inflammation was site specifically and covalently conjugated to the exterior of rAAV6. To achieve conjugation, the scFv was functionalized with an orthogonal click chemistry group. This conjugation utilized site-specific sortase A methodology, thus preserving scFv binding capacity to VCAM-1. The AAV6 was separately functionalized with 4-azidophenyl glyoxal (APGO) via covalent adducts to arginine residues in the capsid's heparin co-receptor binding region. APGO functionalization removed native tropism, greatly reducing rAAV6-GFP transduction into all cells tested, and the effect was similar to the inhibition seen in the presence of heparin. Utilizing the incorporated functionalizations, the scFv was then covalently conjugated to the exterior of rAAV6 via strain-promoted azide-alkyne cycloaddition (SPAAC). With both the removal of native heparin tropism and the addition of VCAM-1 targeting, rAAV6 transduction of endothelial cells was greatly enhanced compared to control cells. Thus, this novel and modular targeting system could have further application in re-directing AAV6 toward inflamed endothelium for therapeutic use.

INTRODUCTION

Gene-based therapies hold great therapeutic potential. While initially considered mostly for monogenic disorders, they are increasingly being investigated for a broader range of complex indications, including neurodegenerative diseases, cancer, and cardiovascular disease.[1] Efficient and safe delivery, however, remains a long-standing and significant challenge,[2] particularly where treatment requires long-term transduction of vascular endothelial cells, as for, e.g., the treatment of atherosclerosis. Currently, recombinant vectors based on the recombinant adeno-associated virus (rAAV) have the best clinical features, in that they are associated with low inflammation and pathogenicity and offer long-term expression.[3] While all available vectors show low endothelial transduction levels, rAAV transduction is particularly low, with 3% of cells being transduced even when clamped in a mouse vessel for 30 min[4] and other experiments suggesting similarly low transduction rates.[5–7] Addressing the challenge of rAAV endothelial transduction, most lines of experimentation have looked at modifying or "reshuffling" the vector capsid through genetic means,[8] utilizing stronger or cell-specific promoters,[9] or focusing on more specific modes of physical delivery.[10] Here, we addressed the challenge by utilizing a novel combination of conjugation methodologies to both de-target an AAV from off-target cells and to actively target it toward inflamed endothelial cells, through vascular cell-adhesion molecule (VCAM-1).

VCAM-1 or CD106 is a type I transmembrane glycoprotein that belongs to the immunoglobulin G (IgG) superfamily and is one of earliest markers of vascular inflammation. In malignant tumors, VCAM-1 is expressed by cancer cells and/or on the cancer-associated vasculature.[11,12] It is also one of the best markers of atherosclerosis, with its strong expression and specific localization making it ideal for imaging and detection.[13] VCAM-1 expression persists throughout the development of atherosclerosis, plays an active role in the associated pathological immune cell recruitment, and is also a marker of the later instability associated with rupture and clinical events.[14] Along with the fact that it is readily accessible in the vasculature, VCAM-1's expression patterns make it an ideal molecule to target gene delivery vectors toward for anti-atherosclerosis as well as anti-cancer

Received 3 April 2019; accepted 2 July 2019;
https://doi.org/10.1016/j.omtm.2019.07.003.

Correspondence: Christoph E. Hagemeyer, PhD, NanoBiotechnology Laboratory, Monash University, Melbourne, VIC, Australia.
E-mail: christoph.hagemeyer@monash.edu
Correspondence: Paul Gregorevic, PhD, Centre for Muscle Research, Department of Physiology, University of Melbourne, Melbourne, VIC, Australia.
E-mail: pgre@unimelb.edu.au

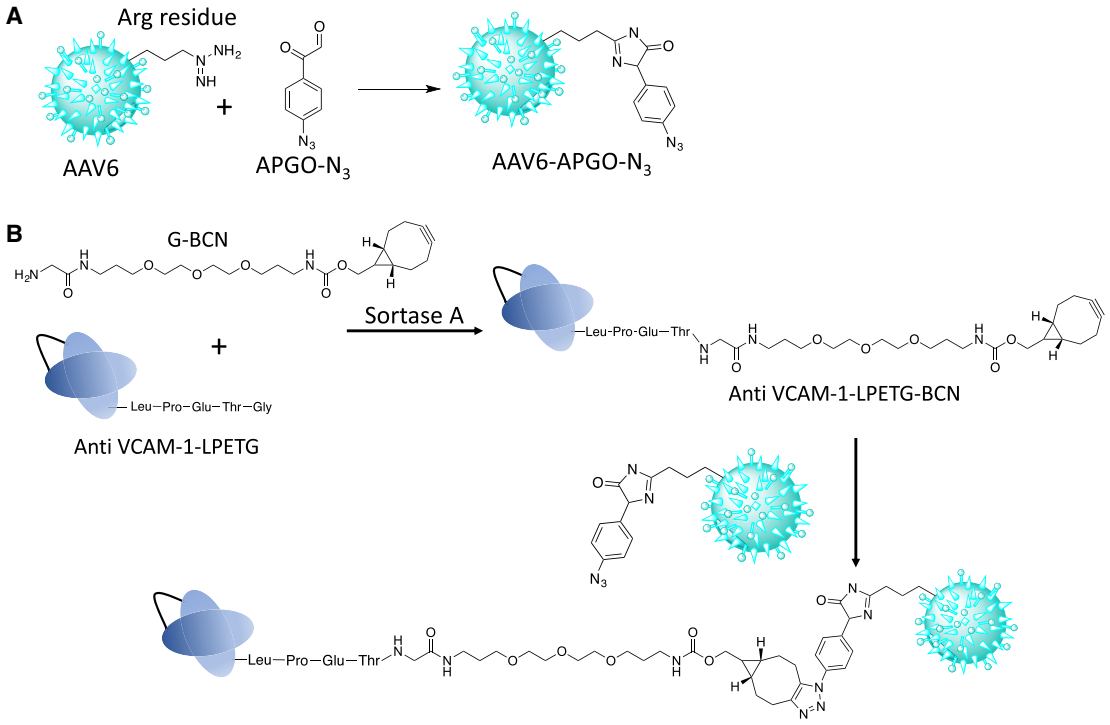

Figure 1. Schematic of the Conjugations

(A) AAV6 was functionalized with APGO to install an azide handle. (B) The scFv-LPETG was functionalized with G-BCN (via sortase A conjugation) such that the two can be joined together with click chemistry.

therapy.[15] Given the recognized requirement for "direct access and high titer" in vascular gene therapy,[16,17] we produced a VCAM-1 binding single-chain antibody (scFv) for attachment to the exterior of an rAAV with the aim of enabling direct binding to inflamed endothelium and enhancing uptake, thereby overcoming the natural 3-min half-life of rAAV6 vectors in circulation.[18]

rAAVs are available in a multitude of different serotypes, each with differing tropisms and capsid structures.[8] Many have strong liver tropism, which is thought to be mediated by heparin binding by a cluster of arginine and other basic residues on the capsid surface.[19,20] Conversely, the same binding to heparin sulfate is reported to sequester entry into endothelial cells.[21] Methylglyoxal (MGO), a natural metabolite of the glycolytic pathway also found in Manuka honey,[22,23] forms hydroimidazolone adducts with lysine and arginine residues.[24,25] Horowitz et al.[26] showed that the external arginine residues could be glycated with MGO. The glycation was shown to block the heparin binding of an rAAV2 vector and in mice resulted in a more widespread transduction away from the liver. rAAV6, thought to be putatively one of the better serotypes for endothelial transduction,[5,7,27,28] contains one of these sites[29,30] and could also be amenable to glycation by MGO.

For this work, we used the azide group containing MGO variant 4-azidophenyl glyoxal (APGO) as a handle for click chemistry. The strain-promoted azide-alkyne cycloaddition (SPAAC)[31] variant of click chemistry is a fast, biorthogonal reaction between an azide group and a ring-strained cyclo-octene, such as BCN (Bicyclo[6.1.0]non--4-yn-9-ol).[32] To incorporate BCN into the anti-VCAM-1 scFv, an enzymatic sortase conjugation, which links together the peptide linkers LPETG and a glycine (G) motif to form a covalent, site-specific bond without disrupting the antibody function,[33,34] could be used to attach G-BCN to an LPETG-tagged anti-VCAM-1 scFv. Thus, rAAV6 could be modified to contain an azide handle with APGO and $scFv_{VCAM}$-LPETG conjugated to G-BCN and the two joined conjugated together via click chemistry (Figure 1).

RESULTS

LPETG-Tagged anti-VCAM-1 scFv Production and Validation

The anti-VCAM-1 scFv used here was originally sequenced from a hybridoma cell line expressing the anti-mouse VCAM-1 monoclonal antibody MK2.7.1 and developed for recombinant bacterial expression.[12,35] Here, the sequence was used to generate a construct optimized for insect cell expression and with the desired tags: $scFv_{VCAM}$V5-LPETG-His_8. The construct was cloned into a new vector: pAc5.1/binding immunoglobulin proteins (BiPs), which combined the properties of two commercially available vectors: pAc5.1 and plasmid metallothionein (pMT)/BiP (Thermo Fisher Scientific), allowing constitutive expression (not requiring copper induction) into the supernatant (Figure S1). The construct was produced via

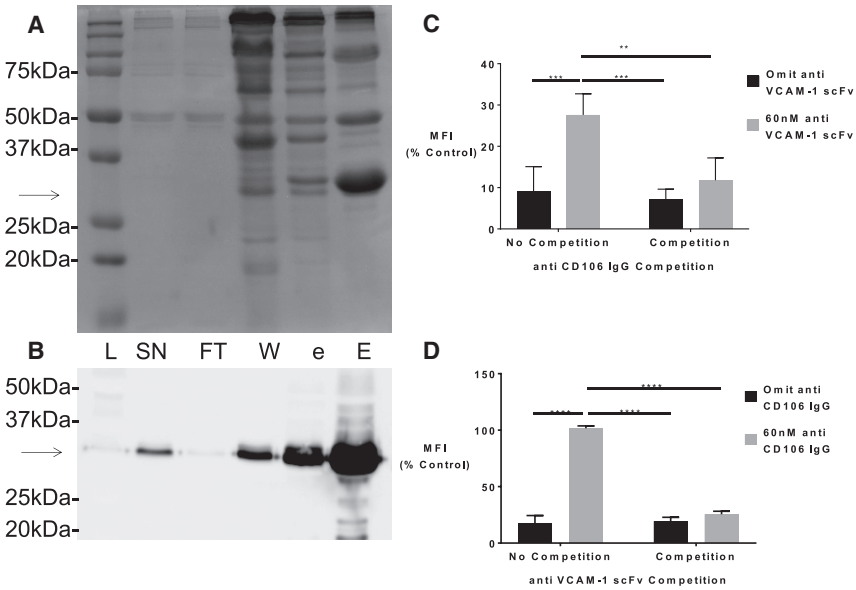

Figure 2. Anti-VCAM-1 scFv Production

(A and B) SDS-PAGE (A) and anti-His tag western blot (B) analysis of anti-VCAM-1 scFv production and purification. L, lane marker; SN, culture supernatant; FT, flow through from column loading; W, wash fraction; e, pre-elution peak; and E, elution peak. The scFv band comes up at 30.5 kDa (indicated by arrow) and increases in intensity over the course of the purification (equal volume was loaded). (C and D) Specific binding of the anti-VCAM-1 scFv to the VCAM-1 on SVEC4-10 cells, as determined using flow cytometry. (C) The anti-VCAM-1 scFv binds to SVEC4-10 cells, as detected by anti His-488 and flow cytometry, and this is competitively inhibited by a 10-fold molar excess of monoclonal anti-CD106 IgG. (D) A 10-fold molar excess of the anti-VCAM-1 scFv can also competitively inhibit the binding of the monoclonal anti-CD106 IgG to SVEC4-10 cells. Data displayed represents four independent replicates, with data normalized to the CD106 IgG control for each experiment. A two-way ANOVA with Tukey's multiple-comparisons correction was carried out. Error bars show SD with *$p < 0.05$, **$p < 0.01$, ***$p < 0.001$, and ****$p < 0.0001$.

dimethyldioctadecyl ammonium bromide (DDAB) transfection of D.Mel2 cells and purified with histidine-tagged affinity chromatography (Figures 2A and 2B). The yield was usually between 1 and 5 mg/L production, and the product could bind to VCAM-1-expressing SVEC4-10 cells, as determined by flow cytometry. Additionally, scFv binding could be both competed by and compete for the binding of a commercially available anti-CD106 (VCAM-1) IgG (Figures 2C and 2D), indicating specificity and potency. Furthermore, binding was tested on mouse heart endothelial cells (MHECs), Chinese hamster ovary (CHO), and HepG2 cells, and the scFv bound well to endothelial VCAM-1-expressing MHEC cells, but not to the non-endothelial CHO or HepG2 cells (Figure S3).

Sortase Conjugation of LPETG-Tagged Anti-VCAM scFv to G-BCN

The produced anti-VCAM-1 scFv with LPETG tag could then be conjugated to G-BCN with sortase enzyme and was further purified by collecting the flow through from a nickel affinity column (removing the His-tagged sortase enzyme and unconjugated anti-VCAM-1 scFv as the sortase reaction removes the His tag on the conjugate). The attachment of G-BCN to the scFv was validated by a reaction with N_3-Cy7.5 dye and visualized on SDS-PAGE to asses both conjugation and product purity (Figure 3A). The binding of the conjugate scFv-BCN compared to scFv alone was assessed with flow cytometry (Figures 3B and S4), and the activity was preserved due to the physiological conditions and site-specific nature of the sortase reaction.

Glycation of AAV6-GFP with APGO to Both Block Native Tropism and Incorporate an Azide Handle

rAAV6-GFP (capable of transducing cells to express GFP) was modified with different concentrations of MGO and APGO and the effect on rAAV6-GFP transduction into CHO-K1 cells assessed (Figure 4A). The effect was concentration dependent and similar between the two compounds. 1 mM MGO and/or APGO showed a significant decrease in transduction in the assay and was used for future conjugation experiments. Horowitz et al.[26] had reported a reduction in antibody recognition following glycation, which would be beneficial for rAAV delivery; however, the reduction was not seen here using anti-AAV6 antibodies and dot blotting (Figure S6). The interplay between heparin and MGO/APGO was also assessed in a gene transduction assay on CHO-K1, HepG2, SVEC4-10, and MHEC cells. Heparin pre-incubation or MGO modification was shown to decrease AAV6-GFP transduction into these cell types (not significant for SVEC4-10), and when both heparin and MGO/APGO were combined, there was an additive effect, although not statistically significant (Figure S7).

Click Chemistry to Attach the BCN Functionalized Anti-VCAM-1 scFv to the Exterior of the APGO (Azide) Functionalized AAV6

Conjugations with APGO-treated AAV6 were carried out with biotin-BCN, and later the $scFv_{VCAM}$-BCN, to determine optimal conditions. The conjugations were monitored by western blotting with streptavidin-horseradish peroxidase (HRP) (biotin) or anti-V5-HRP (scFv) to detect conjugate at the same size as the rAAV6 capsid proteins (VP1, 87 kDa; VP2, 72 kDa; and VP3, 62 kDa in a 1:1:10 ratio).[30,36] Using this, successful conjugation of both biotin-BCN and $scFv_{VCAM}$-BCN to APGO functionalized AAV6 could be determined (Figures 4B, 4C, and 5A). It appeared that the smaller biotin-BCN bound preferentially to the larger, less abundant capsid proteins, and the $scFv_{VCAM}$-BCN to the smaller, more abundant VP3 protein, although never exclusively. Co-labeling was possible, although pre-conjugation with scFv inhibited biotin binding to some extent. Overall, the optimal binding conditions were determined with 5 μM $scFv_{VCAM}$-BCN; greater concentrations resulted in non-specific

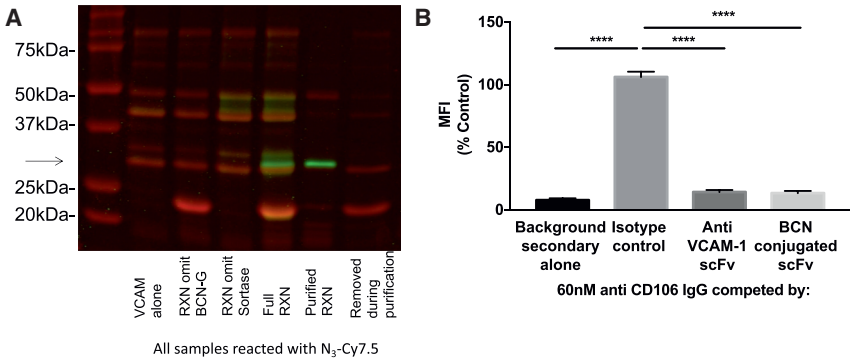

Figure 3. Sortase Conjugation of LPETG-Tagged Anti-VCAM-1 scFv to G-BCN

(A) Odyssey scanned gel showing sortase reaction, controls, and clean-up step. Protein is in red and Cy7.5 dye in green. Presence of Cy7.5 dye at the correct height for scFv (30 kDa, indicated by arrow) indicates successful conjugation and is seen in the full reactions alone. RXN indicates reaction. (B) Anti-VCAM-1 scFv binding to SVEC4-10 cells is unimpeded following sortase conjugation, as shown by a 10-fold molar excess of conjugated and unconjugated scFv competitively inhibiting anti-CD106 IgG binding equivalently. Isotype control indicates competition (or lack thereof) by a non-binding control scFv. Data is from three independent experiments, and data was normalized to the CD106 IgG-positive control in each experiment. A one-way ANOVA with Tukey's multiple comparisons correction was used. Error bars show SD with *$p < 0.05$, **$p < 0.01$, ***$p < 0.001$, and ****$p < 0.0001$.

(non-azide dependent) binding and less insufficient conjugation, as evident on the blots 4b and c.

In Vitro Validation of VCAM-1 Targeted AAV6-GFP

AAV6-GFP conjugated to the anti-VCAM-1 scFv using the above methodologies was dialyzed to remove excess scFv, and the effect on GFP gene transduction in endothelial VCAM-1-expressing SVEC4-10 and MHEC cells and non-endothelial non-VCAM-1-expressing HepG2 and CHO cells was assessed. Note that the expression of VCAM-1 in these cells is validated in Figure S3. Both long (2 days; Figure 5B) and short (1 h; Figure 5C) incubations with cells were investigated, and unmodified AAV6-GFP was used as a normalization control for each cell type and time point. In all cells and time points, the APGO-alone treatment of AAV6-GFP drastically reduced transduction compared to untreated control in the same cell type. For the extended incubation time, the addition of the anti-VCAM-1 scFv to the APGO-treated AAV6-GFP improved transduction in SVEC4-10 cells, and to a much greater extent in MHEC cells, but not in control HepG2 and CHO cells. In the reduced incubation setting, more relevant to physiological administration, the addition of the anti-VCAM-1 scFv to the APGO-treated AAV6-GFP greatly enhanced transduction of both SVEC4-10 and MHEC cells, and again not in control cells. The improved transduction in the reduced incubation setting could be partially inhibited by competition with an excess of the scFv during transduction (Figure S9), indicating active targeting.

DISCUSSION

Using our novel approach combining rAAV6, APGO, click chemistry, sortase conjugation, and the anti-VCAM-1 scFv, rAAV6 gene transduction could be decreased in all cells through the use of MGO or APGO and specifically rescued in VCAM-1 expressing SVEC4-10 and MHEC endothelial cells through the addition of the anti-VCAM-1 scFv. The effect was more pronounced with the more physiologically relevant shorter exposure and could be partially competitively inhibited, indicating active targeting. Given the accessibility of the vasculature and the benefit longer retention has on rAAV transduction, the observed VCAM-1-mediated anchoring could allow specific transduction at sites of inflammation in the vasculature (such as atherosclerosis and cancer) even at early stages. Given the challenging nature of endothelial transduction for all vector types, the targeting is therefore a significant advantage.

Our experiments represent the first use of MGO with rAAV6, as opposed to the previously used rAAV2, and opens the possibility that other AAV serotypes with a heparin-binding region could be modified in the same way. Trialing other serotypes could have interesting implications in terms of their modified tropisms, both with and without the click chemistry attachment of a targeting agent. Horowitz et al.[26] had already observed an *in vivo* reduction in liver and other tropisms with their MGO-modified rAAV2, and this was mirrored in our experiments, where transduction was significantly reduced in all cell types. The tropism change gives the advantage of potentially reducing off-target transduction in other organs and even within the vasculature itself. The MGO-induced reduction in antibody recognition seen by Horowitz et al.[26] would have clinical advantages through reducing the neutralizing antibody response to the rAAV[37] but was not seen here. The difference in results is possibly due to one of the binding sites of the antibody used in their assessment being the heparin binding site,[38] creating an artificial result, which was not the case here. rAAV6 has a lower prevalence of neutralizing antibodies in the human population than AAV2, giving it an advantage here.[39]

Previous studies have utilized the heparin binding site to genetically incorporate targeting agents into rAAV2. Incorporation has been achieved by screening a library of peptides inserted at the heparin binding site[20,40] or incorporating known peptides.[41,42] These types of modifications have the advantage of being a singular component that achieves both de-targeting and re-targeting; however, the production yields and packaging quality of the novel vectors are often low, the insertion is limited in size to peptides, conformation constraints and interactions with the capsid site means they do not always target or even block heparin binding as expected (hence the screening approach), and the system is not flexible, being difficult to establish,

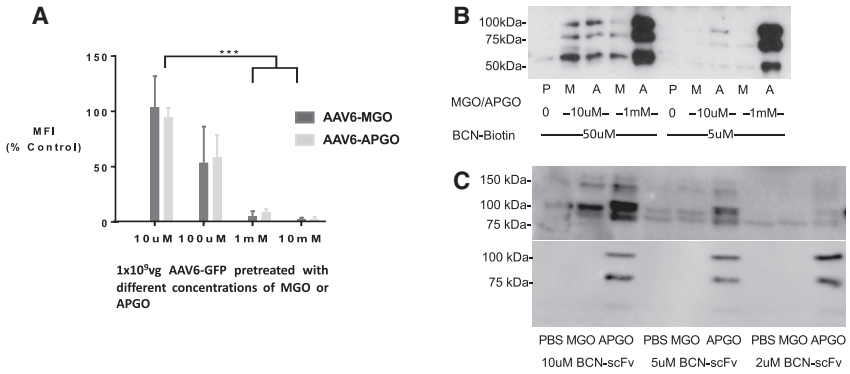

Figure 4. Optimization of the System Components

(A) Effect of different concentrations of MGO and APGO treatment on AAV6-GFP transduction of CHO cells. CHO cells were transduced with 1 × 10^9 vg AAV6-GFP, which had received pre-treatment with MGO or APGO (concentration as specified) and the resulting cell GFP expression (mean fluorescent intensity) after 48 hr measured with flow cytometry. Data is from three independent experiments (run in triplicate) and was normalized to 1 × 10^9 vg untreated AAV6-GFP control for each experiment. (Note, for visual clarity, stars representing $p < 0.05$ were omitted here.) A two-way ANOVA with Tukey's multiple-comparisons test was carried out. Error bars show SD with *$p < 0.05$, **$p < 0.01$, ***$p < 0.001$, and ****$p < 0.0001$. See Figure S5 for titration controls. (B and C) Titrations of click conjugations to APGO-AAV6, as shown by western blotting. (B) AAV6 treated with different concentrations of APGO and negative controls PBS and MGO were conjugated with different concentrations of BCN-biotin. Equal volumes were run on a streptavidin-HRP western blot detecting biotin conjugation product at sizes corresponding to the AAV6 capsid proteins. P, PBS treated negative control; M, MGO negative control; and A, APGO. (C) AAV6 treated with 1 mM APGO and negative controls PBS and MGO were conjugated with different concentrations of BCN-scFv and also subsequently to BCN-biotin as a positive control. Equal volumes were run on an anti-V5-HRP western blot (top panel) detecting scFv at sizes corresponding to AAV6 capsid protein plus scFv and stripped and re-probed with streptavidin-HRP (bottom panel). Note the relevant protein sizes: scFv, 30.5 kDa; VP1, 87 kDa; VP2, 72 kDa; VP3, 62 kDa. No loading control was used, as the samples are prepared equivalently and are not cell lysates.

limited to the AAV serotype used, and meaning improvements in the affinity are not easily achieved.[43,44]

More modular and indirect approaches have also been trialed, also at the AAV heparin binding site. Stachler et al.[44] inserted a biotin ligase sequence into the AAV1 heparin region and Liu et al.[45] an aldehyde tag into the AAV2 site, both allowing modular attachments of targeting agents. Similar to our approach, these offer the advantage that the targeting agent can be indirectly and site specifically added to the system, preserving its function, and the choice of targeting agent is flexible and interchangeable. They do, however, retain the caveat of requiring genetic modification of the vector, carrying the same difficulties as above, including affecting production titer and packaging quality and being inflexible by serotype.[44–46]

Along these lines, our initial approach was actually to engineer the GGGWW sortase tag into the VP2 capsid protein at the N terminus, as this is a requirement for the enzyme.[47] The VP2 N terminus is the other common rAAV site to be modified, and various studies have inserted tags,[48] targeting agents,[49] and even a scFv at this site,[50] so it is known to be modifiable and found on the exterior. We encountered issues with the typical difficulties involved in these types of modifications, including upsetting the capsid protein ratios and structure, decreasing transduction, and subsequently also constraints with the optimal concentrations for sortase reactions. Modifications at the VP2 N terminus also do not allow de-targeting, merely targeting on top of native tropism.

Click chemistry has previously been used to attach targeting agents to adenoviruses,[32,51] which can be metabolically labeled to contain azide groups in a way that AAV cannot, but to our knowledge our experiments are the first use of click chemistry and/or sortase conjugation with rAAV. Despite the biotin-BCN and scFv-BCN showing background binding to the rAAV6 at higher concentrations, which has been reported before for click reactions on other substrates,[52] the use of click chemistry and sortase in our approach allows controlled, biocompatible, and covalent attachment. As used together previously, the sortase step enables the incorporation of targeting biomolecules in a site-directed and gentle enzymatic manner without affecting their targeting capacity, while the use of ring-strained click chemistry allows fast, catalyst-free biorthogonal attachment.[32,53,54]

Combining sortase enzyme and click chemistry with rAAV6 glycation provides an efficient, flexible, and controlled way for the generation of targeted rAAV vectors. While MGO has been previously used to change tropism of rAAV2, the use of APGO to allow azide-based conjugation and actively retarget an rAAV is novel. Our approach offers the advantage that it does not require genetic modification of the vector, enables both de- and re-targeting, controlled attachment, is gentle on all components, and is entirely modifiable and flexible. The three-step protocol means that the components can be produced separately, using the most efficient production method for each component. This is of particular importance to the rAAV6, as the standard vector can be produced with no effect on titer or packaging. The three-step protocol also means that the most beneficial reaction type for each component and the most efficient ratios for each reaction can be used. It also allows intermediate purifications to obtain defined reaction partners. Where direct production of BCN-tagged targeting agents is possible a two-step system could be used (e.g., with BCN-biotin), and labeling to allow tracking or further modified targeting would also be possible. Lastly, the serotype and/or targeting agent can easily be substituted, meaning the conjugation strategy could be used as a discovery tool or tailored to suit other biological challenges. Overall, as all the components required for our system are easily interchangeable, a highly flexible platform technology for targeted gene transfer was established.

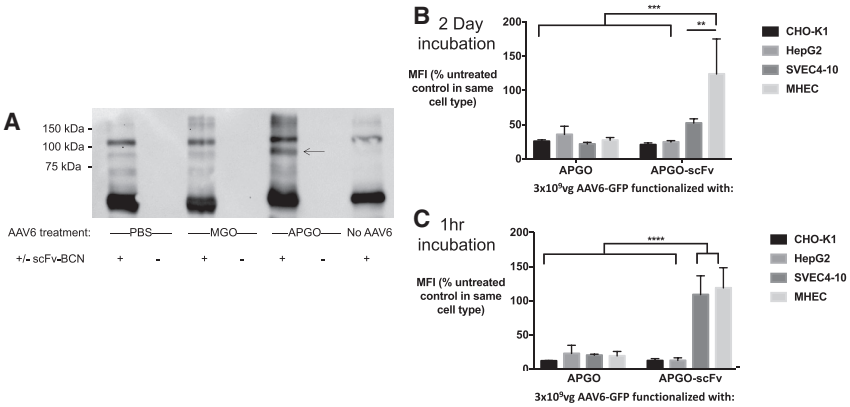

Figure 5. Functional Testing of the Assembled anti-VCAM-1 Targeted AAV6

(A) Western blot showing optimized click conjugation of scFv-BCN to APGO-AAV6. Conjugation product is indicated by an arrow (found with APGO-AAV6 + scFv-BCN only) and is absent in all negative controls (omit scFv samples and PBS- and MGO-treated AAV6). Equal sample volumes were run on a western blot using anti-V5-HRP, detecting scFv at sizes corresponding to AAV6 capsid protein plus scFv (scFv, 30.5 kDa; VP1, 87 kDa; VP2, 72 kDa; VP3, 62 kDa), indicating covalent conjugation. Please note other bands represent background scFv, as indicated by the scFv-only negative control. No loading control was used, as the samples are prepared equivalently and are not cell lysates. (B and C) Gene transduction assay showing the effect of APGO treatment alone and APGO-mediated anti-VCAM-1 targeting on AAV6-GFP transduction into two endothelial and two non-endothelial cell types. 3×10^9 vg AAV6-GFP was incubated with cells for 2 days, and subsequently the cell GFP expression was measured by flow cytometry (B) or the AAV6-GFP was incubated with cells for 1hr before being removed and replaced with fresh media and the GFP expression measured 2 days later (C). All data was normalized to untreated AAV6-GFP in the same cell type and time grouping for each of the three independent replicates run in triplicate. A two-way ANOVA with Tukey's multiple comparisons correction was used. Error bars show SD with *$p < 0.05$, **$p < 0.01$, ***$p < 0.001$, and ****$p < 0.0001$. See Figures S8–S10 for additional controls and information.

MATERIALS AND METHODS

Cell Culture

SVEC4-10 cells were purchased from the American Type Culture Collection (Manassas, VA, USA) and CHO-K1 cells from DSMZ (Braunschweig, Germany). Both were maintained in DMEM (Gibco), supplemented with 10% fetal calf serum (FCS), 2 mM L-glutamine, 50 U/mL penicillin and streptomycin, and 1× non-essential amino acids. HepG2 cells were a gift from Dr. Brian Drew (Baker Institute, Melbourne, Australia) and cultured in low-glucose DMEM with the same supplements. MHEC cells were a gift from Prof. Harshal Nandurkar (Monash University, Melbourne, Australia) and were cultured on flasks pre-coated with 0.5% gelatin and in EBM-2 (Lonza) with the accompanying BulletKit of supplements. All above cells were cultured at 37°C with 5% CO_2. D.Mel-2 cells were purchased from Thermo Fisher Scientific and were grown in Express 5 serum-free media (Gibco) supplemented with 16.5 mM L-glutamine and 50 U/mL penicillin/streptomycin, with 120 rpm shaking and atmospheric CO_2. Cultures were maintained between 2×10^6 and 20×10^6 cells/mL.

Anti-VCAM-1 scFv Production

The commercial plasmid pAc5.1 (Invitrogen) was modified to create pAc5.1BiPss. This has the advantage that the expressed protein is secreted to the medium and not trapped in the cells, causing issues with aggregation and insoluble inclusion bodies. For this step, the BiP sequence was amplified from the commercial plasmid pMT (Invitrogen) via standard PCR with flanking KpnI and *NotI* restriction sites. This was subcloned into pAc5.1 using the same restriction sites and transformed into NEB Turbo competent cells. Isolated plasmids were sent for sequencing at the Australian Genome Research Facility, and the Emboss Needle sequence alignment tool (EMBL-EBI) was used to confirm a match with the expected sequence.

The anti-mouse VCAM-1 scFv construct, including V5 tag, LPETG tag, His_8 tag, and codon optimized for insect cell expression, and flanked by the restriction sites *NcoI* and *NotI*, was ordered from GeneArt and supplied in the plasmid mammalian (pMA). This was subcloned into pAc5.1BiPss using the same restriction sites and transformed into NEB Turbo competent cells. Colony screening PCR was used to determine successful ligation, using a forward primer flanking the insertion site and the reverse primer binding internal to the construct. Identified plasmids were sent for sequencing at the Australian Genome Research Facility. Primers flanked the insertion site, allowing full sequence coverage, and the Emboss Needle sequence alignment tool (EMBL-EBI) was used to confirm a match with the expected sequence. For expression in insect cells, plasmid DNA was amplified from a glycerol stock using an Endofree QIAGEN plasmid maxi kit. See Figure S1.

DNA was transfected into D.Mel-2 cells using a lipid-based transfection described by Han.[55] In brief, 160 µg plasmid was first incubated in supplemented Express 5 serum-free media with 100 µg/mL DDAB (Sigma Aldrich) for 30 min at room temperature. This was then added to 1 L culture at 2×10^6 cells/mL media and incubated for 5 days. Cells were then centrifuged at 16,000 × *g* for 20 min and the recovered supernatant filtered through a 40-µm membrane (Merck Millipore) prior to purification on a Bio-Rad BioLogic fast protein liquid chromatography (FPLC) system (Bio-Rad Laboratories). The sample was loaded onto a HisTrap excel column (GE Healthcare life sciences) pre-equilibrated in wash buffer (50 mM NaH_2PO_4, 300 mM NaCl, pH 8) at a flow rate of 5 mL/min. Following loading, the column was washed in eight column volumes wash buffer containing 30 mM imidazole and then product eluted in eight column volumes wash buffer containing 250 mM imidazole. The elution peak was detected with a Quad Tech detector measuring absorbance at 280 nm, and the product was dialyzed in a 10-kDa molecular weight cut-off

(MWCO) membrane overnight against PBS, with two buffer changes prior to analysis and downstream use.

Non-binding control scFv (anti-Her2 scFv) used in some experiments was produced using the same methods.

G-BCN

This orthogonal linker was made as described previously.[53]

Sortase Conjugation

The produced $scFv_{VCAM}$V5-LPETG-His_8 was conjugated to G-BCN using the enzymatic sortase conjugation. Sortase enzyme was produced in-house as described previously.[34] 10 μM $scFv_{VCAM}$V5-LPETG-His_8, 30 μM sortase enzyme, and 300 μM G-BCN were reacted together in 50 mM Tris, 150 mM NaCl, 0.5 mM $CaCl_2$ (pH 8) at 37°C for 4 hr with shaking. Excess sortase and unreacted scFv was then removed by passing through a QIAGEN Ni-NTA Superflow column (1 mL). Excess G-BCN was subsequently removed by dialysis against PBS in a 10-kDa MWCO membrane.

ScFv Quality Control

To determine scFv presence and purity, collected scFv fractions were analyzed with Coomassie-stained SDS-PAGE (12% acrylamide) and/or western blotting with an anti-His_6 HRP monoclonal IgG conjugate used at 0.0125 U/mL for 1 hr (Sigma-Aldrich). 30 μL samples were used for SDS-PAGE and 10 μL samples for western blotting. To asses sortase reactions, 30 μL samples of conjugates and controls thereof were reacted with a large excess (30 μM) N_3-Cy7.5 (azide-Cy7.5 dye, Lumiprobe) for 1 hr at room temperature prior to immediate loading dye addition and boiling, and stored at −20°C until SDS-PAGE analysis. These samples were imaged on an LI-COR Odyssey scanner.

The concentration of dialyzed samples was determined using a Direct Detect infrared spectrometer system (Merck Millipore) or BCA assay (Pierce) for lower concentration (less than 0.2 mg/mL) samples.

To determine scFv activity, VCAM-1 expressing SVEC4-10 cells at 250,000 cells per fluorescence-activated cell sorting (FACS) tube in 50 μL PBS were incubated with between 2 and 20 ng/μL scFv (60–600 nM) for 10 min. Cells were then washed in 0.5 mL PBS and resuspended in 50 μL 1:50 diluted anti-penta His Alexa Fluor 488 conjugate (QIAGEN) for 15 min, prior to further washing and resuspension in 300 μL PBS for flow cytometry analysis. 60 nM anti-mouse CD106 IgG, raised in rat (BioLegend), followed by 1:50 diluted fluorescein isothiocyanate (FITC)-conjugated AffiniPure goat anti-rat IgG (Jackson ImmunoResearch Laboratories) was used as a positive control. For competition assays to determine specificity or alternatively binding of sortase conjugates no longer containing a His tag, the competitor was added to cells at 600 nM for 10 min prior to primary antibody addition at 60 nM. Samples were run on a FACS-Calibur, the SVEC4-10 cells were gated from the forward scatter (FSC)/side scatter (SSC) plot, and data from 10,000 cells within the gated population was collected. Data was analyzed using FlowJo V10.1 and mean fluorescence intensity (MFI) in the FL-1 channel was used as the primary quantitative readout. For experiments involving SVEC4-10 cells, only MFI was always normalized to the anti-CD106 IgG-positive control (as VCAM-1 expression on the SVEC4-10 cells varied from experiment to experiment). Where the positive control was used in statistics, a separate reading was taken from the normalization control. MHEC, CHO, and HepG2 cells were treated equivalently except that in experiments involving all cells the data was not normalized to the positive control antibody, as this did not bind to the negative control cells, and the interest was in relative expression between cells. The isotype control scFv was an anti-Her2 scFv produced using the same expression system and methods.

AAV6-eGFP Production

AAV6-eGFP was produced as described previously.[9] In brief, HEK293 cells were co-transfected with the plasmids pDGM6 and plasmid adeno-associated virus (pAAV; carrying EGFP), and the cell lysates collected after 3 days and purified on a heparin affinity column. Vector titers were measured by quantitative dot blotting.

Dot Blotting

AAV6-eGFP with and without MGO or APGO treatment was prepared in serial dilution (2×10^9 vg for highest sample), and 2-μL samples were dotted onto nitrocellulose membrane and allowed to dry. Blotting was carried out as per standard protocols with anti-AAV6 antibodies ADK1a and b derived from hybridoma cell lines[56] and subsequently 1:5,000 diluted goat anti-mouse HRP.

MGO Treatment

MGO and APGO were purchased from Sigma Aldrich. For initial experiments, 10 μM–10 mM, and as preparation for conjugations, 1 mM of each (or PBS control), was mixed with 1×10^{12} vg/mL AAV6-eGFP overnight at room temperature, similar to Horowitz et al.[26] The 100-μL samples were then dialyzed against 1 mL PBS, with two buffer changes, in a Slide-A-Lyzer MINI dialysis device, 10 kDa MWCO, 100 μL (Thermo Fisher Scientific), and used immediately or stored at −80°C.

Click Reactions

APGO-treated AAV6 and MGO- and PBS-treated controls, prepared as above, were diluted 5-fold into desired final concentration BCN-biotin or BCN_{scFv}VCAM (BCN conjugated anti-VCAM-1 scFv) and reacted at room temperature for 3 hr. For the targeted gene transduction assay, a concentration of 5 μM BCN_{scFv}VCAM was used, and subsequently the sample was dialyzed against PBS in a Micro Float-A-Lyzer dialysis device, 100 kDa MWCO (Spectrum), overnight at 4°C, with two buffer changes. For western blotting samples, no cleanup step was included, and for the co-labeling experiments, the 3 hr, 5 μM BCN_{scFv}VCAM incubation was followed by 50 μM BCN-biotin for 30 min. Western blot samples were run on SDS-PAGE (8% acrylamide) and blotted with streptavidin-HRP (protein conjugate, BD Biosciences) 1: 30,000 dilution, 1 hr incubation for biotin samples, or Anti-V5-HRP (monoclonal IgG conjugate, Invitrogen) 1: 15,000 dilution, 1 hr incubation for BCN_{scFv}VCAM samples.

Gene Transduction Assay and Targeting Assays

Cells (CHO-K1, HepG2, SVEC4-10, and MHEC) were plated out in 12-well plates at 100,000 cells/mL/well. After allowing adherence overnight, the media was removed and replaced with media lacking FCS (and also lacking the heparin supplement in the case of the MHEC cells). 3×10^9 vg (targeting experiments) or 1×10^9 vg (all other experiments) AAV6-GFP with the treatments and attachments of interest was then added and incubated for 2 days prior to harvesting with trypsin-EDTA and analyzing GFP expression with flow cytometry (with the same settings for all cells and measuring mean FL-1 as per the scFv activity assay). Heparin and anti-VCAM-1 scFv inhibition (300 nM) were added 30 min prior to AAV6-GFP. For targeting experiments, scFv inhibition and AAV6-GFP addition was in 0.5 mL media lacking FCS, and after 1 hr AAV6-GFP incubation, the media was removed and replaced with 1 mL fresh media for the 2-day incubation prior to flow cytometry. Each of the three independent replicates were carried out with three technical replicates, and the MFI of these was averaged and normalized to an unmodified and/or untreated AAV6-GFP standard within each replicate.

Statistics

All graphs display means of independent replicates and error bars the standard deviation. One- or two-way ANOVAs, as indicated, with Tukey's multiple-comparisons correction were conducted using GraphPad Prism. Normalized data were considered unmatched, while non-normalized data matched, to account for interexperimental differences in the baseline. Unless specified, all data in the figure were compared to all other data in the figure. *$p < 0.05$, **$p < 0.01$, ***$p < 0.001$, ****$p < 0.0001$.

SUPPLEMENTAL INFORMATION

Supplemental Information can be found online at https://doi.org/10.1016/j.omtm.2019.07.003.

AUTHOR CONTRIBUTIONS

H.A.P. had a lead role in data curation, formal analysis, investigation, validation, and writing of the original draft; H.Q. had a supporting role in investigation and validation; T.U.C., D.H., and C.G. each had a supporting role in investigation and validation; P.S.D. had a supporting role in funding acquisition, investigation, project administration, and validation; K.P. had a supporting role in investigation; P.G. had a supporting role in funding acquisition, investigation, project administration, and validation; C.E.H. had a lead role in data curation, funding acquisition, formal analysis, investigation, project administration, validation, and writing of the original draft.

CONFLICTS OF INTEREST

The authors declare no competing interests.

ACKNOWLEDGMENTS

This work was funded by the National Health and Medical Research Council (NHMRC), the Australian Research Council (ARC), and the National Heart Foundation of Australia (NHF). The work was also supported in part by the Victorian Government's Operational Infrastructure Support Program. We thank Prof. Kleinschmidt for the anti-AAV producing hybridoma cell lines.

REFERENCES

1. Sheridan, C. (2011). Gene therapy finds its niche. Nat. Biotechnol. *29*, 121–128.
2. Verma, I.M., and Somia, N. (1997). Gene therapy – promises, problems and prospects. Nature *389*, 239–242.
3. Mingozzi, F., and High, K.A. (2011). Therapeutic in vivo gene transfer for genetic disease using AAV: progress and challenges. Nat. Rev. Genet. *12*, 341–355.
4. Vassalli, G., Büeler, H., Dudler, J., von Segesser, L.K., and Kappenberger, L. (2003). Adeno-associated virus (AAV) vectors achieve prolonged transgene expression in mouse myocardium and arteries in vivo: a comparative study with adenovirus vectors. Int. J. Cardiol. *90*, 229–238.
5. Sen, S., Conroy, S., Hynes, S.O., McMahon, J., O'Doherty, A., Bartlett, J.S., Akhtar, Y., Adegbola, T., Connolly, C.E., Sultan, S., et al. (2008). Gene delivery to the vasculature mediated by low-titre adeno-associated virus serotypes 1 and 5. J. Gene Med. *10*, 143–151.
6. Seiler, M.P., Miller, A.D., Zabner, J., and Halbert, C.L. (2006). Adeno-associated virus types 5 and 6 use distinct receptors for cell entry. Hum. Gene Ther. *17*, 10–19.
7. Chen, S., Kapturczak, M., Loiler, S.A., Zolotukhin, S., Glushakova, O.Y., Madsen, K.M., Samulski, R.J., Hauswirth, W.W., Campbell-Thompson, M., Berns, K.I., et al. (2005). Efficient transduction of vascular endothelial cells with recombinant adeno-associated virus serotype 1 and 5 vectors. Hum. Gene Ther. *16*, 235–247.
8. Asokan, A., Schaffer, D.V., and Samulski, R.J. (2012). The AAV vector toolkit: poised at the clinical crossroads. Mol. Ther *20*, 699–708.
9. Gregorevic, P., Blankinship, M.J., Allen, J.M., Crawford, R.W., Meuse, L., Miller, D.G., Russell, D.W., and Chamberlain, J.S. (2004). Systemic delivery of genes to striated muscles using adeno-associated viral vectors. Nat. Med. *10*, 828–834.
10. Wolfram, J.A., and Donahue, J.K. (2013). Gene therapy to treat cardiovascular disease. J. Am. Heart Assoc. *2*, e000119.
11. Kong, D.H., Kim, Y.K., Kim, M.R., Jang, J.H., and Lee, S. (2018). Emerging Roles of Vascular Cell Adhesion Molecule-1 (VCAM-1) in Immunological Disorders and Cancer. Int. J. Mol. Sci. *19*, E1057.
12. Dienst, A., Grunow, A., Unruh, M., Rabausch, B., Nör, J.E., Fries, J.W., and Gottstein, C. (2005). Specific occlusion of murine and human tumor vasculature by VCAM-1-targeted recombinant fusion proteins. J. Natl. Cancer Inst. *97*, 733–747.
13. Broisat, A., Toczek, J., Dumas, L.S., Ahmadi, M., Bacot, S., Perret, P., Slimani, L., Barone-Rochette, G., Soubies, A., Devogdt, N., et al. (2014). 99mTc-cAbVCAM1-5 imaging is a sensitive and reproducible tool for the detection of inflamed atherosclerotic lesions in mice. J. Nucl. Med *55*, 1678–1684.
14. Libby, P. (2002). Inflammation in atherosclerosis. Nature *420*, 868–874.
15. Nahrendorf, M., Keliher, E., Panizzi, P., Zhang, H., Hembrador, S., Figueiredo, J.L., Aikawa, E., Kelly, K., Libby, P., and Weissleder, R. (2009). 18F-4V for PET-CT imaging of VCAM-1 expression in atherosclerosis. JACC Cardiovasc. Imaging *2*, 1213–1222.
16. Baker, A.H., Kritz, A., Work, L.M., and Nicklin, S.A. (2005). Cell-selective viral gene delivery vectors for the vasculature. Exp. Physiol. *90*, 27–31.
17. Schultz, B.R., and Chamberlain, J.S. (2008). Recombinant adeno-associated virus transduction and integration. Mol. Ther *16*, 1189–1199.
18. Fargnoli, A.S., Katz, M.G., Yarnall, C., Sumaroka, M.V., Stedman, H., Rabinowitz, J.J., Koch, W.J., and Bridges, C.R. (2011). A pharmacokinetic analysis of molecular cardiac surgery with recirculation mediated delivery of βARKct gene therapy: developing a quantitative definition of the therapeutic window. J. Card. Fail. *17*, 691–699.
19. Opie, S.R., Warrington, K.H., Jr., Agbandje-McKenna, M., Zolotukhin, S., and Muzyczka, N. (2003). Identification of amino acid residues in the capsid proteins of adeno-associated virus type 2 that contribute to heparan sulfate proteoglycan binding. J. Virol. *77*, 6995–7006.
20. Müller, O.J., Leuchs, B., Pleger, S.T., Grimm, D., Franz, W.M., Katus, H.A., and Kleinschmidt, J.A. (2006). Improved cardiac gene transfer by transcriptional and transductional targeting of adeno-associated viral vectors. Cardiovasc. Res. *70*, 70–78.

21. Pajusola, K., Gruchala, M., Joch, H., Lüscher, T.F., Ylä-Herttuala, S., and Büeler, H. (2002). Cell-type-specific characteristics modulate the transduction efficiency of adeno-associated virus type 2 and restrain infection of endothelial cells. J. Virol. *76*, 11530–11540.

22. Atrott, J.H.T. (2009). Methylglyoxal in Manuka Honey - Correlation with Antibacterial Properties. Czech J. Food Sci. *27*, S163–S165.

23. Thornalley, P.J. (1996). Pharmacology of methylglyoxal: formation, modification of proteins and nucleic acids, and enzymatic detoxification–a role in pathogenesis and antiproliferative chemotherapy. Gen. Pharmacol. *27*, 565–573.

24. Takahashi, K. (1977). The reactions of phenylglyoxal and related reagents with amino acids. J. Biochem. *81*, 395–402.

25. Lo, T.W., Westwood, M.E., McLellan, A.C., Selwood, T., and Thornalley, P.J. (1994). Binding and modification of proteins by methylglyoxal under physiological conditions. A kinetic and mechanistic study with N alpha-acetylarginine, N alpha-acetylcysteine, and N alpha-acetyllysine, and bovine serum albumin. J. Biol. Chem. *269*, 32299–32305.

26. Horowitz, E.D., Weinberg, M.S., and Asokan, A. (2011). Glycated AAV vectors: chemical redirection of viral tissue tropism. Bioconjug. Chem. *22*, 529–532.

27. Zincarelli, C., Soltys, S., Rengo, G., and Rabinowitz, J.E. (2008). Analysis of AAV serotypes 1-9 mediated gene expression and tropism in mice after systemic injection. Mol. Ther *16*, 1073–1080.

28. Grimm, D., Kay, M.A., and Kleinschmidt, J.A. (2003). Helper virus-free, optically controllable, and two-plasmid-based production of adeno-associated virus vectors of serotypes 1 to 6. Mol. Ther *7*, 839–850.

29. Wu, Z., Asokan, A., Grieger, J.C., Govindasamy, L., Agbandje-McKenna, M., and Samulski, R.J. (2006). Single amino acid changes can influence titer, heparin binding, and tissue tropism in different adeno-associated virus serotypes. J. Virol. *80*, 11393–11397.

30. Ng, R., Govindasamy, L., Gurda, B.L., McKenna, R., Kozyreva, O.G., Samulski, R.J., Parent, K.N., Baker, T.S., and Agbandje-McKenna, M. (2010). Structural characterization of the dual glycan binding adeno-associated virus serotype 6. J. Virol. *84*, 12945–12957.

31. Sletten, E.M., and Bertozzi, C.R. (2011). From mechanism to mouse: a tale of two bioorthogonal reactions. Acc. Chem. Res. *44*, 666–676.

32. Dommerholt, J., Schmidt, S., Temming, R., Hendriks, L.J., Rutjes, F.P., van Hest, J.C., Lefeber, D.J., Friedl, P., and van Delft, F.L. (2010). Readily accessible bicyclononynes for bioorthogonal labeling and three-dimensional imaging of living cells. Angew. Chem. Int. Ed. Engl. *49*, 9422–9425.

33. Schwarz, M., Katagiri, Y., Kotani, M., Bassler, N., Loeffler, C., Bode, C., and Peter, K. (2004). Reversibility versus persistence of GPIIb/IIIa blocker-induced conformational change of GPIIb/IIIa (alphaIIbbeta3, CD41/CD61). J. Pharmacol. Exp. Ther. *308*, 1002–1011.

34. Ta, H.T., Prabhu, S., Leitner, E., Jia, F., von Elverfeldt, D., Jackson, K.E., Heidt, T., Nair, A.K., Pearce, H., von Zur Muhlen, C., et al. (2011). Enzymatic single-chain antibody tagging: a universal approach to targeted molecular imaging and cell homing in cardiovascular disease. Circ. Res. *109*, 365–373.

35. Gottstein, C., Wels, W., Ober, B., and Thorpe, P.E. (2001). Generation and characterization of recombinant vascular targeting agents from hybridoma cell lines. Biotechniques *30*, 190–194, 196, 198 passim.

36. Rose, J.A., Maizel, J.V., Jr., Inman, J.K., and Shatkin, A.J. (1971). Structural proteins of adenovirus-associated viruses. J. Virol. *8*, 766–770.

37. Calcedo, R., Vandenberghe, L.H., Gao, G., Lin, J., and Wilson, J.M. (2009). Worldwide epidemiology of neutralizing antibodies to adeno-associated viruses. J. Infect. Dis. *199*, 381–390.

38. Wobus, C.E., Hügle-Dörr, B., Girod, A., Petersen, G., Hallek, M., and Kleinschmidt, J.A. (2000). Monoclonal antibodies against the adeno-associated virus type 2 (AAV-2) capsid: epitope mapping and identification of capsid domains involved in AAV-2-cell interaction and neutralization of AAV-2 infection. J. Virol. *74*, 9281–9293.

39. Boutin, S., Monteilhet, V., Veron, P., Leborgne, C., Benveniste, O., Montus, M.F., and Masurier, C. (2010). Prevalence of serum IgG and neutralizing factors against adeno-associated virus (AAV) types 1, 2, 5, 6, 8, and 9 in the healthy population: implications for gene therapy using AAV vectors. Hum. Gene Ther. *21*, 704–712.

40. Perabo, L., Büning, H., Kofler, D.M., Ried, M.U., Girod, A., Wendtner, C.M., Enssle, J., and Hallek, M. (2003). In vitro selection of viral vectors with modified tropism: the adeno-associated virus display. Mol. Ther. *8*, 151–157.

41. White, K., Büning, H., Kritz, A., Janicki, H., McVey, J., Perabo, L., Murphy, G., Odenthal, M., Work, L.M., Hallek, M., et al. (2008). Engineering adeno-associated virus 2 vectors for targeted gene delivery to atherosclerotic lesions. Gene Ther. *15*, 443–451.

42. White, S.J., Nicklin, S.A., Büning, H., Brosnan, M.J., Leike, K., Papadakis, E.D., Hallek, M., and Baker, A.H. (2004). Targeted gene delivery to vascular tissue in vivo by tropism-modified adeno-associated virus vectors. Circulation *109*, 513–519.

43. Varadi, K., Michelfelder, S., Korff, T., Hecker, M., Trepel, M., Katus, H.A., Kleinschmidt, J.A., and Müller, O.J. (2012). Novel random peptide libraries displayed on AAV serotype 9 for selection of endothelial cell-directed gene transfer vectors. Gene Ther. *19*, 800–809.

44. Stachler, M.D., Chen, I., Ting, A.Y., and Bartlett, J.S. (2008). Site-specific modification of AAV vector particles with biophysical probes and targeting ligands using biotin ligase. Mol. Ther *16*, 1467–1473.

45. Liu, Y., Fang, Y., Zhou, Y., Zandi, E., Lee, C.L., Joo, K.I., and Wang, P. (2013). Site-specific modification of adeno-associated viruses via a genetically engineered aldehyde tag. Small *9*, 421–429.

46. Nicklin, S.A., Buening, H., Dishart, K.L., de Alwis, M., Girod, A., Hacker, U., Thrasher, A.J., Ali, R.R., Hallek, M., and Baker, A.H. (2001). Efficient and selective AAV2-mediated gene transfer directed to human vascular endothelial cells. Mol. Ther *4*, 174–181.

47. Ton-That, H., Mazmanian, S.K., Faull, K.F., and Schneewind, O. (2000). Anchoring of surface proteins to the cell wall of *Staphylococcus aureus*. Sortase catalyzed in vitro transpeptidation reaction using LPXTG peptide and NH(2)-Gly(3) substrates. J. Biol. Chem. *275*, 9876–9881.

48. Asokan, A., Johnson, J.S., Li, C., and Samulski, R.J. (2008). Bioluminescent virion shells: new tools for quantitation of AAV vector dynamics in cells and live animals. Gene Ther. *15*, 1618–1622.

49. Münch, R.C., Janicki, H., Völker, I., Rasbach, A., Hallek, M., Büning, H., and Buchholz, C.J. (2013). Displaying high-affinity ligands on adeno-associated viral vectors enables tumor cell-specific and safe gene transfer. Mol. Ther *21*, 109–118.

50. Yang, Q., Mamounas, M., Yu, G., Kennedy, S., Leaker, B., Merson, J., Wong-Staal, F., Yu, M., and Barber, J.R. (1998). Development of novel cell surface CD34-targeted recombinant adenoassociated virus vectors for gene therapy. Hum. Gene Ther. *9*, 1929–1937.

51. Oum, Y.H., and Carrico, I.S. (2012). Altering adenoviral tropism via click modification with ErbB specific ligands. Bioconjug. Chem. *23*, 1370–1376.

52. van Geel, R., Pruijn, G.J., van Delft, F.L., and Boelens, W.C. (2012). Preventing thiol-yne addition improves the specificity of strain-promoted azide-alkyne cycloaddition. Bioconjug. Chem. *23*, 392–398.

53. Alt, K., Paterson, B.M., Westein, E., Rudd, S.E., Poniger, S.S., Jagdale, S., Ardipradja, K., Connell, T.U., Krippner, G.Y., Nair, A.K., et al. (2015). A versatile approach for the site-specific modification of recombinant antibodies using a combination of enzyme-mediated bioconjugation and click chemistry. Angew. Chem. Int. Ed. Engl. *54*, 7515–7519.

54. Leung, M.K., Hagemeyer, C.E., Johnston, A.P., Gonzales, C., Kamphuis, M.M., Ardipradja, K., Such, G.K., Peter, K., and Caruso, F. (2012). Bio-click chemistry: enzymatic functionalization of PEGylated capsules for targeting applications. Angew. Chem. Int. Ed. Engl. *51*, 7132–7136.

55. Han, K. (1996). An efficient DDAB-mediated transfection of Drosophila S2 cells. Nucleic Acids Res. *24*, 4362–4363.

56. Kuck, D., Kern, A., and Kleinschmidt, J.A. (2007). Development of AAV serotype-specific ELISAs using novel monoclonal antibodies. J. Virol. Methods *140*, 17–24.